

KINETIC ANALYSIS OF THERMAL DECOMPOSITION OF SPIROBORATE ESTER OF CURCUMIN WITH MALONIC ACID

¹Jeena John, ¹Sudha Devi Rugmini and ³Balachandran Sreedharan Nair*

¹Department of Chemistry, Mahatma Gandhi College, Thiruvananthapuram, Kerala.

^{2,*}Principal, NSS College Ottapalam, Kerala, Thiruvananthapuram

Abstract

Spiroborate ester of curcumin with malonic acid was synthesized by condensation of curcumin, boric acid and malonic acid. The synthesized complex was characterized by different spectral techniques. The isothermal thermogravimetric method was used to study the thermal decomposition of spiroborate ester of curcumin with malonic acid at the heating rate of 10 °C/min in nitrogen atmosphere. Coats Redfern method was used to study the order of thermal degradation. Freeman Carrol, Coats Redfern and Sharp Wentworth method were used to calculate the thermal activation energy, entropy change, free energy change and frequency factor. The kinetic parameters calculated using above mentioned methods is in good agreement with each other. The kinetic parameters of this complex were compared with those reported for similar spiroborate esters in literature in order to study the effect of lactone ring in the thermal stability of spiroborate esters.

Key words

Spiroboronate esters; thermogravimetry; order of thermal decomposition; activation energy.

1. Introduction

Tetra coordinated boron complexes, commonly called as spiroboranes, have recently attracted extensive attention due to their various application in analytical and biological fields¹⁻¹¹. Spiroboranes display outstanding electronic and optical properties have found application in organic photovoltaic¹⁻², OLED display³, lasing⁴, nonlinear optics⁵, cell imaging⁶, photodynamic therapy⁷ etc. They also find application in lithium batteries, wood preservatives, catalysis⁸⁻⁹, linker molecule in biological samples¹⁰, reagent for chromatographic separation of saccharides¹¹ etc.

Curcumin in acid medium reacts with boric acid to form a red colored 2:1 complex called rosocyanin¹². Yellow color of curcumin changes to red color on complexation with boron. This color reaction is used for the estimation of boron in various matrices in different fields like nuclear energy, metallurgy, pharmacy and agriculture¹²⁻¹⁴. Different derivatives of rosocyanin can be prepared by replacing one molecule curcumin with dicarboxylic or alpha hydroxy acids. Malonic acid is a better alternative for preparing its derivative¹⁵. The spiroborate esters of curcumin are known for its less hydrolytic stability and this property make them a suitable candidate for the carriers of curcumin for drug delivery. Curcumin boron complex with oxalic acid (rubrocurcumin) is well studied and its thermal stability studies were reported¹⁶. Spiroborate esters of curcumin with malonic acid (CBMO) have structural features similar to rubrocurcumin and thus a promising molecule to use as a better alternate for rubrocurcumin, the knowledge on thermal stability contribute in this regards.

The present paper deals with the synthesis and structural characterization of spiroborate ester of curcumin with malonic acid (CBMO). A systematic investigation of the thermal decomposition of CBMO was done by Coats Redfern (CR), Freeman Carrol (FC) and Sharp Wentworth (SW) methods. Energy of activation (E_a), frequency factor (A) and thermodynamic parameters viz. enthalpy of activation (ΔH^\ddagger), entropy of activation (ΔS^\ddagger) and free energy of activation (ΔG^\ddagger) associated with the thermal degradation were also determined using

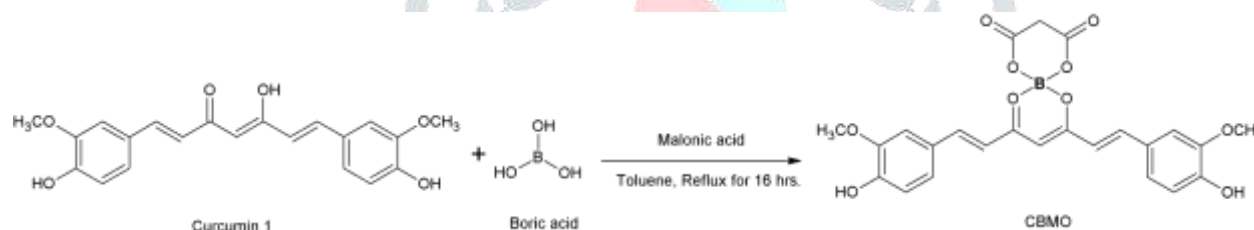
these methods. The order of thermal degradation (n) was determined by applying CR method. The thermal stability of CBMO was compared with other similar spiroborate esters reported in literature by the same group.

2. Experimental Procedure

Malonic acid and boric acid used for the preparation of complex were analytical grade from SDS Mumbai. The chemicals and reagents used in this study were of analytical and reagent quality. The purity of the prepared complex was ascertained by TLC for which a glass plate coated with silica gel was used as stationary phase and 9:1 chloroform methanol mixture as eluent. UV spectra were recorded on Elico 198 Biospectrophotometer. IR spectra were obtained in KBr pellet on Perkin Elmer IR spectrophotometer. ^1H , ^{13}C and ^{11}B NMR spectra were recorded in DMSO on Bruker Avance NMR spectrometer operating at 500 MHz. Thermogravimetric analyses were recorded on Perkin-Elmer Thermogravimetric Analyzer in dynamic nitrogen atmosphere (100 mL/min) with a heating rate of $10\text{ }^\circ\text{C}/\text{min}$ in the temperature range of $40\text{-}750\text{ }^\circ\text{C}$. The commercial sample of curcumin contains mainly three curcuminoids which include curcumin, demethoxycurcumin (DMC) and bisdemethoxycurcumin (BDMC). Column chromatography was used for the separation of curcumin from other curcuminoids¹⁷⁻¹⁸.

2.1. Preparation of CBMO

A mixture of column chromatographically purified curcumin (0.01 M), boric acid (0.01 M), and malonic acid (0.01 M) in 10 mL toluene were heated under reflux using a Dean-Stark trap for 16 hrs. The reaction was monitored through TLC and after the completion of the reaction the solvent was removed through filtration to get the solid product¹⁹. It was further washed with toluene to remove unreacted curcumin (Scheme 1) and purified by flash chromatography using chloroform-methanol mixture as solvent.



Scheme 1. Synthesis of CBMO

2.2. The spectral data of CBMO

Yield 80%; UV λ_{max} = 516 nm (acetonitrile); IR (KBr) : 3512 (OH), 1670 (C=O in lactone ring), 1513 (C=O in curcumin), 1207 (C-O in phenol), 1058 cm^{-1} (C-O in OCH₃); ^1H NMR (400 MHz, DMSO-*d*₆); δ 3.84 (s, 6H, OCH₃), 3.70 (s, 2H, CH₂) 6.48 (s, 1H, CH), 7.36 (d, *J* = 10Hz, 2H, Ar-H), 6.89 (d, *J* = 8Hz, 2H, Ar-H), 7.45 (s, 2H, Ar-H), 8.02 (d, *J* = 15.6Hz, 2H, =CH), 7.07 (d, *J* = 15.6Hz, 2H, =CH), 10.175 (s, 2H, OH); ^{13}C NMR: 55.76, 100.47, 112.59, 116.03, 117.30, 125.73, 126.01, 148.21, 148.27, 151.86, 165.55, 177.58.

3. Results and discussion

The synthesized CBMO was dark brown powder with 80 % yield and found stable at room condition. It is soluble in solvents like acetonitrile, acetone, methanol etc. and in these solvent it shows wine red color. In dipolar aprotic solvent like acetonitrile and acetone CBMO is stable however in protic solvent methanol it hydrolyze slowly to form curcumin. Addition of water in any of these solvents decreases its hydrolytic stability as shown by color fading with time.

3.1. UV-Vis spectral studies

The UV-Vis spectra of curcumin and CBMO were recorded in acetonitrile medium at room temperature. This red shift from 420 nm of curcumin to 516 nm region for CBMO is due to the $\pi\text{-}\pi^*$ electron transfer from

oxygen to boron atom during complex formation²⁰. The molar extinction coefficient (ϵ) obtained for CBMO is $7.12 \times 10^4 \text{ M}^{-1}\text{cm}^{-1}$.

3.2. IR Spectral studies

In the IR spectra of CBMO the strong band due to the hydrogen bonded carbonyl functional group of curcumin in the region 1628 cm^{-1} red shifted to 1513 cm^{-1} similar to metal complexes of curcumin²¹⁻²². In CBMO the boron is attached to two rings that formed by curcumin and malonic acid and oriented perpendicular to each other and thus called spiro²³. The lactone ring formed by the esterification of malonic acid, the C=O group of that ring have a stretching frequency at 1670 cm^{-1} . The peak at 1157 cm^{-1} can be ascribed to the antisymmetric stretching frequency of the BO_4 tetrahedron of CBMO²⁴. A broad asymmetric band at 3476 cm^{-1} , indicate the presence of phenolic groups of curcumin that are not involved in condensation reaction.

3.3. NMR spectral studies

In the ^1H NMR spectra of CBMO the peak corresponding to enolic -OH at 16.05 ppm in curcumin disappears in the spectra of CBMO, which indicate curcumin chelates to boron by the keto-enol moiety. The chemical shifts values of other hydrogen atoms correspond to that of curcumin²⁵ which show a slight change after its coordination with boron. The ^1H NMR signal in the region δ 3.7 and 3.8 ppm is of methoxy group, at δ 10.17 ppm is of Ar-OH group, the multiple peak in the range δ 7.03 to 7.45 ppm is due to Ar-H, doublet peak at δ 6.87 and 7.98 ppm is due to CH=CH protons, and a peak at δ 6.48 ppm is due to single hydrogen. The chemical shift values of the CH_2 group of coordinated malonate group appeared at δ 3.70 ppm in CBMO. In the ^{13}C NMR spectra of CBMO the chemical shift value corresponds to the curcumin shows trivial change after coordination with boron²⁶. Two new peaks at δ 177.58 and 126.01 ppm were observed and is due to -CO and - CH_2 group of lactone ring respectively.

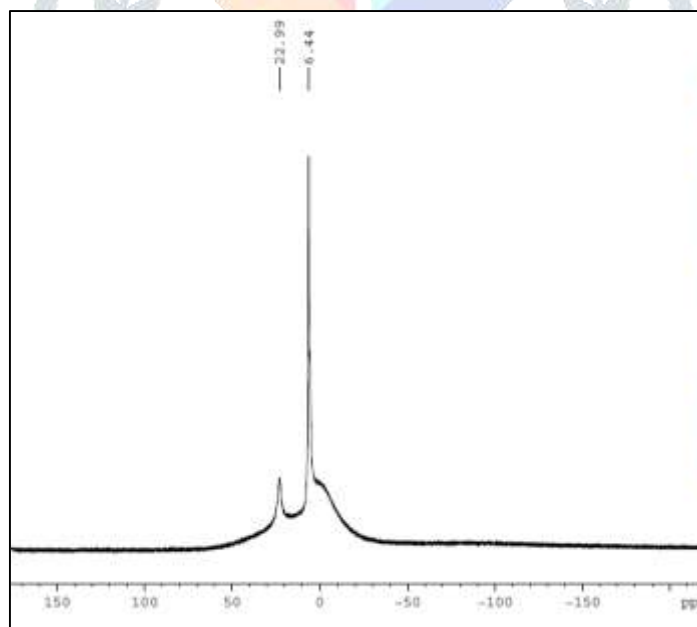


Figure. 1 ^{11}B NMR spectrum of CBMO

^{11}B NMR spectra give direct evidence for boron complexation. The ^{11}B NMR spectrum of CBMO is given in figure 1. For tetrahedral boron attached to six member rings a peak in the range 6 to 6.73 ppm is expected²⁷ and in the present case a strong peak at 6.44 ppm is observed. The weak peak at 22.99 ppm may be due to the borate moiety formed due to the hydrolysis of the complex in methanol solution which is reported in the range 22.52 to 23.19 ppm²⁸.

3.4. Thermal decomposition of CBMO

The TGA of CBMO was carried out from room temperature to 750 °C in nitrogen atmosphere. The TG-DTG curve are shown in figure 2 and the data from the thermogravimetric analysis reveal that CBMO decomposes in two stages. An initial decomposition was seen in the temperature range 280-321°C, and it is due to the loss of malonate group with a weight loss of 17.92/17.88 % (calcd. /found). This stage follows a continuous weight loss from 321-700 °C due to the curcumin degradation. The final product in the thermal decomposition may be the B₂O₃. The thermal decomposition steps were shown in figure 3. The thermal degradation of curcumin starts at 190 °C indicating that the boron complexation increased its thermal stability²⁹.

A similar degradation pattern is observed for rubrocurcumin where the first degradation stage is the removal of oxalate group in the temperature range 287-305 °C which follows the degradation of curcumin moiety from 305 °C³⁰. The comparable initial decomposition temperature for the complexes indicates similar thermal stability for rubrocurcumin and CBMO.

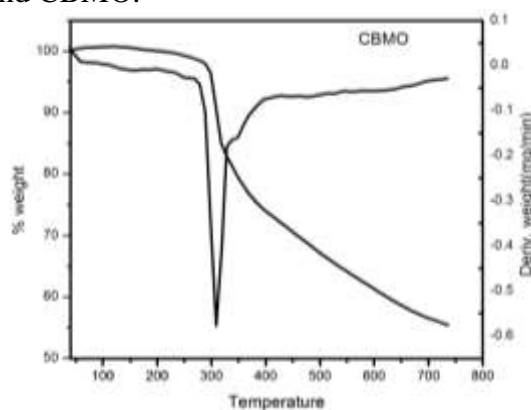


Figure 2 The TG-DTG curve for the thermal decomposition of CBMO

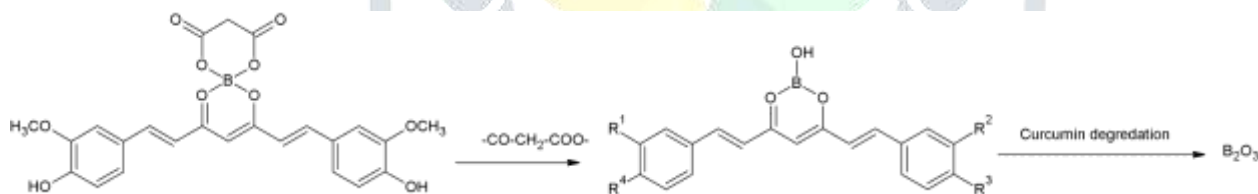


Figure 3 Thermal decomposition of CBMO

3.5. Kinetic analysis of thermal degradation

3.5.1. Theoretical aspects

Kinetic parameters for the thermal decomposition of CBMO were determined by analyzing the TGA data using CR, SW and FC methods. The mathematical expression for CR method³¹ is

$$\ln \left[\frac{1-(1-\alpha)^{1-n}}{(1-n)T^2} \right] = \ln \frac{AR}{\beta E} \left[1 - \frac{2RT}{E_a} \right] - \frac{E_a}{RT} \quad (1)$$

Where $\alpha = \frac{w_0 - w_t}{w_0 - w_f}$, w_0 is the initial mass of the sample, w_t is the mass of the sample at temperature T , w_f is the final mass at temperature at which the mass loss is approximately unchanged. E_a is the activation energy of the degradation, A is the pre-exponential factor, R is the universal gas constant, n is the order of reaction, β is the heating rate. A plot of LHS of the equation 1 against $1/T$ was drawn. From the slope of this plot, the energy of activation E_a was calculated. Frequency factor A was calculated from the intercept.

SW relation used to evaluate the degradation kinetics is³²

$$\ln \left[\frac{(dc/dt)}{(1-c)} \right] = \ln \left(\frac{A}{\beta} \right) - [Ea/RT] \quad (2)$$

Where dc/dt is the rate of change of fraction of weight with change in temperature. By plotting a graph between $\ln \left[\frac{(dc/dt)}{(1-c)} \right]$ versus $1/T$ should be a straight line which gives Ea from its slope.

FC relation used to evaluate the degradation kinetics is³³

$$\ln \left[\frac{dw/dt}{w_r} \right] = \ln A - \frac{Ea}{RT} \quad (3)$$

Where dw/dt is the rate of change of weight with time, $w_r = w_c - w$ and w is the fraction of weight loss at time t and w_c is the weight loss at the completion of the reaction. By plotting the graph between $\ln \left[\frac{dw/dt}{w_r} \right]$ versus $1/T$ should be a straight line for decomposition following first order kinetics with a slope of $(-Ea/R)$ and A was obtained from the intercept on former axis.

$\Delta H^\#$, $\Delta S^\#$, and $\Delta G^\#$ associated with the thermal degradation were calculated using the equation³⁴

$$\Delta H^\# = Ea - RT \quad (4)$$

$$\Delta S^\# = R \left[\ln \left(\frac{Ah}{kT} \right) - 1 \right] \quad (5)$$

$$\Delta G^\# = \Delta H^\# - T\Delta S^\# \quad (6)$$

3.5.2. Reaction Order calculation

The exact order of thermal decomposition can be determined by using CR method by plotting $\ln \left[\frac{1-(1-\alpha)^{1-n}}{(1-n)T^2} \right]$ vs. $1/T$. R^2 value is computed using the least square method for the straight line plots obtained by plotting different values of n ranging from $n=0$ to 2. The n value which gave the best fit value i.e., $R^2 \sim 1$ represents the order of thermal degradation. The data given in table 1 clearly indicates the order of thermal degradation is 1.4.

Table 1. Calculated R^2 values for different values of n in CR method.

n	R^2	n	R^2
0.1	0.9389	1.1	0.9926
0.2	0.9468	1.2	0.9943
0.3	0.9547	1.3	0.9953
0.4	0.9626	1.4	0.9957
0.5	0.9703	1.5	0.9955
0.6	0.9776	1.6	0.9946
0.7	0.9835	1.7	0.9932
0.8	0.9860	1.8	0.9912
0.9	0.9762	1.9	0.9888
1	0.9903	2	0.9859

The kinetic and thermodynamic parameters viz. energy of activation (Ea), frequency factor (A), entropy change of activation ($\Delta S^\#$), enthalpy change of activation ($\Delta H^\#$) and free energy change of activation ($\Delta G^\#$) were calculated using CR, FC and SW isoconversional methods in order to compare the values obtained from these methods. Representative plots of $\ln[g(\alpha)/T^2]$ versus $1/T$ for CR method, $\ln[(dc/dt)/(1-c)]$ versus $1/T$ for SW method and $\ln[(dw/dt)/w_r]$ versus $1/T$ for FC method were shown in figure 4. The parameters obtained for each method are tabulated in table 2. The R^2 value calculated using three methods were found to lie in the range 0.9871-0.9900 showing good fit with the linear function. The calculated Ea value lie in the range 483.42

for CR method, 451.03 for SW method and 456.28 for FC method. It was observed that the difference in the values of E_a calculated using three different methods are relatively small. The high E_a values indicate high thermal stability of CBMO. The positive value of ΔH^\ddagger means that the decomposition processes are endothermic in nature and the positive ΔS^\ddagger value showed that the reaction is fast. The value of ΔG^\ddagger is positive indicating the non-spontaneous nature of reaction³⁵.

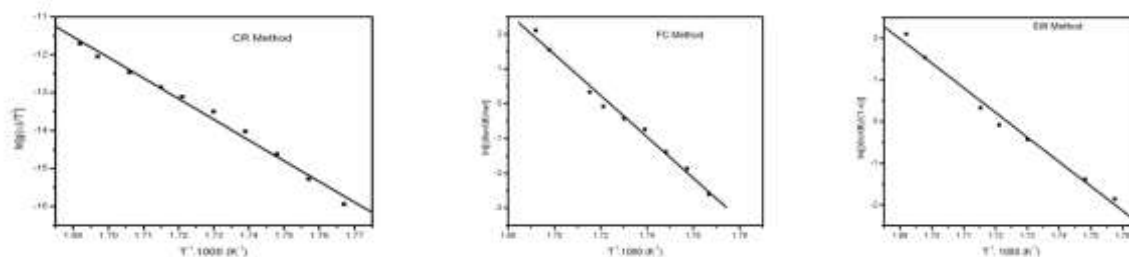


Figure 4 CR, FC and SW plots for the thermal decomposition of CBMO.

Table 2. Kinetic parameters calculated using CR, FC and SW methods.

Methods	R^2	E_a	A	ΔH^\ddagger	ΔS^\ddagger	ΔG^\ddagger
		(kJ mol ⁻¹)	(s ⁻¹)	(kJ mol ⁻¹)	(J K ⁻¹ mol ⁻¹)	(kJ mol ⁻¹)
CR	0.9957	483.42	4.97×10^{41}	478.58	539.46	171.63
FC	0.9871	456.28	1.18×10^{41}	451.55	527.67	151.30
SW	0.9881	451.03	1.96×10^{40}	447.57	515.37	233.17

3.5.3. Influence of ligand on thermal stability

The E_a value of the complex is expected to increase with increasing thermal stability of compounds³⁶. The literature E_a values of CBMO analogues rubrocurcumin, rosocyanin and spiroborate ester of curcumin with salicylic acid (CBS) determined by CR, FC and SW methods is summarized in table 3^{16,35, 37-38}. The stability order of these compounds based on E_a value is rubrocurcumin > CBMO > CBS > rosocyanin. The highest E_a value observed is for rubrocurcumin, spiroborate ester formed from oxalic acid and second highest value observed is for CBMO. Both the compounds are formed from dicarboxylic acid which indicates that the spiroborate esters formed from dicarboxylic acids are more stable than others. The better stability of rubrocurcumin over CBMO is related to the size of the lactone ring and as the ring size increases the stability decreases³⁹. Among CBMO and CBS, the CBMO is more stable and may due to the presence of two ester bonds in lactone ring. In CBS one of the bond is ester bond since it is formed from an α -hydroxy acid. In rosocyanin, the boron atom is attached to rings formed from curcumin moiety which may have strong steric repulsion and result in least stability.

Table 3. Activation energy values for spiroborate esters of curcumin.

Compound	Lactone ring formed from	E_a (kJ mol ⁻¹)		
		CR method	FC method	SW method

CBMO	Malonic acid	483.42	456.28	451.03
Rubrocurcumin ³⁰	Oxalic acid	683.19	615.92	653.05
Rosocyanin ³⁷	Curcumin	89.59	74.96	--
CBS ³⁸	Salicylic acid	225.44	214.71	214.71

4. Conclusion

The spiroborate ester of curcumin with malonic acid was prepared and its structure was ascertained by various spectral techniques. The synthesized complex was found to be stable upto 287 °C. The order of degradation $n=1.4$ calculated using CR method satisfy both FC and SW method with good approximation hence confirm the order of degradation as 1.4. The values of activation energy calculated using CR, FC and SW methods were in good agreement with each other. High value of frequency factor and positive value of entropy of activation indicates faster reaction rate for thermal decomposition. This was further supported by the high value of frequency factor. The E_a value obtained for CBMO were compared with other spiroborate esters reported earlier and found that ring size and steric effect influences the thermal stability of these compounds.

Acknowledgements

One of the authors (JJ) is thankful to CSIR, New Delhi for awarding Senior Research Fellowship for financial assistance. The authors are also thankful to SAIF, Cochin for carried out the thermal analysis.

References

- Bura, T. Leclerc, N. Fall, S. Leveque, P. Heiser, T. Retailleau, P. Rihn, S. Mirloup, A. and Ziessel, R. 2012. *J Am Chem Soc*; 134: 17404-17407.
- Chambon, S. D'Aleo, A. Baffert, C. Wantz, G. and Fages, F. 2013. *Chem Commun*; 49: 3555-3557.
- Bonardi, L. Kannan, H. Camerel, F. Jolinat, P. Retailleau, P. and Ziessel, R. 2008. *Adv Funct Mater*; 18: 401-413.
- Banuelos, J. Martin, V. Gomez-Duran, C. F. A. Cordoba, I. J. A. Pena-Cabrera, E. Garcia Moreno, I. Costela, A. Perez-Ojeda, M. E. Arbeloa, T. and Arbeloa, I. L. 2011. *Chem Eur J*; 17: 7261-7270
- Hales, J. M. Matchak, J. Barlow, S. Ohira, S. Yesudas, K. Bredas, J. L. and Perry, J. W. 2010. *Science*; 327: 1485-1488.
- Ojida, A. Sakamoto, T. Inoue, M. Fujishima, S. Lippens, G. and Hamachi, I. 2009. *J Am Chem Soc*; 131: 6543-6548.
- Adarsh, N. Avirah, R. R. and Ramaiah, D. 2010. *Org Lett*; 12: 5720-5723.
- Christopher, M. V. and Stephen, A. W. 2011. *Chem Soc Rev*; 40: 1446-1458.
- Stepanenko, V. Jesus, M. D. Correa, W. Guzman, I. Vazquez, C. de la Cruz, W. Marciales, M. O. and Barnes, C. L. 2007. *Tetrahedron Lett*; 48(33): 5799-5802.
- Dembitsky, V. M. Smoum, R. Al-Quntar, A. A. Ali, H. A. Pergament, I. Srebnik, M. 2002. *Plant Science*; 163: 931-942.
- Muynck, C. D. Beauprez, J. Soetaert, W. and Vandamme, E. J. 2006. *Journal of Chromatography A*; 1101: 115-121.
- Spicer, C. P. and Strickland, J. D. H. 1952. *J Chem Soc*; 4644-4650.
- Thangavel, S. Dhavile, S. M. and Dash, K. 2004. *Anal Chim Acta*; 502: 265-270.
- Dyrssen, D.W. Novikov, Y. P. and Uppstrom, L. R. 1972. *Anal Chem Acta*; 60: 139-151.

15. Vijayalaxmi, R. Sathyanarayana, M. N. and Rao, M. V. L. *Ind. J. Chem*; 20B: 907.
16. John, J. Sudha Devi, R. and Balachandran, S. *Acta Cienc. Indica*; XLII C, No. 2: 121-131.
17. Asha, R. Sudha Devi, R. Priya Rajan, S. Balachandran, S. Mohanan, P. V. and Annie Abraham. 2012. *Chem Biol Drug Des*; 80: 887-892.
18. Somparan, P. Phisalaphong, C. and Nakornchai, S. 2007. *Biol Pharm Bull*; 30(1): 74-78.
19. Sui, Z. Salto, R. Li, J. Craik, C. and Paul R Ortiz de Montellano. 1993. *Bioorg Med chem*; 1(6): 415-422.
20. Bai, G. Yu, C. Cheng, C. Hao, E. Wei, Y. Mu, X. and Jiao. L. 2014. *Org. Biomol. Chem*; 12: 1618-1626.
21. Priya, R. S. Balachandran, S. Daisy, and J. Mohan, P V. 2015. *Univers. J. Phy. Appl*; 3: 6-16.
22. Zhao, X. Z. Jiang, T. Wang, L. Yang, H. Zhang, S. and Zhou, P. 2010. *J. Mol. Struct*; 984, 316-325.
23. John, J. Sudha Devi, R. and Balachandran, S. 2015. *J. Acad. Chem. Trs*; 1(2), 24-32.
24. Naumov, P. Zugik, M. Lee, A. and Ng, S W. 2009. *Maced. J. Chem. Chem. Eng.* 28(1), 55-77.
25. Portes, E. Gardrat, C. and Castellan, A. 2007. *Tetrahedron*; 63, 9092-9099.
26. Balaban, A. T. Parkanyi, C. Ghiviriga, I. Aaron, J. Zuzana Zajickova, and B. E. Martinez, O R. 2008. *Arkovic*; 13, 1-9.
27. Kose, D. A. and Zumreoglu-Karan, B. 2012. *Chem. Pap*; 66: 54-60.
28. John, J. Sudha Devi, R. and Balachandran, S. 2018. *Int. J. Chem. Kinet*; 50: 164-177.
29. Chen, Z. Xia, Y. Liao, S. Huang, Y. Li, Y. Hea, Y. Tong, Z. and Li, B. 2014. *Food Chem.* 155: 81-86.
30. John, J. Sudha Devi, R. and Balachandran, S. 2016. *Acta Cienc. Indica*; XLII C. No. 2: 121-131.
31. Coats, A. W. and Redfern, J. P. 1964. *Nature*; 201: 68-69.
32. Sharp, J. B. and Wentworth, S. A. 1969. *Anal Chem*; 41: 2060-2062.
33. Freeman, E. S. and Carroll, B. 1958. *J Chem Rev*; 62: 394-397.
34. Asadi, M. Asadi, Z. Savaripoor, N. Dusek, M. Eigner, V. Shorkaei, M. R. and Sedaghat, M. 2015. *Spectrochimica Acta Part A: Mol Biomol Spectroscopy*; 136: 625-634.
35. John, J. Sudha Devi, R. Balachandran, S. and Babu, KVD. 2017. *J Therm Anal Calorim*; 130: 2301-2314.
36. Mohamed, G. G. Zayed, E. M. and Hindy, A. M. M. 2015. *Spectrochim Acta Part A: Mol Biomol Spectrosc*; 145: 76-84.
37. John, J. Sudha Devi, R. and Balachandran, S. 2017. *Acta Cienc. Indica*; XLIII C: 67-73.
38. John, J. Sudha Devi, R. and Balachandran, S. 2017. *Orient. J. Chem*; 33(2): 849-858.
39. Lorber, G. and Pizer, R. 1976. *Inorg. Chem*; 15: 978-980.